

# Luminescent Probe of Copper–Thiolate Cluster Formation within Mammalian Metallothionein

Anna Rae Green, Anthony Presta, Zbigniew Gasyna,<sup>†</sup> and Martin J. Stillman\*

Department of Chemistry, The University of Western Ontario, London, Ontario, Canada N6A 5B7

Received April 28, 1994\*

Emission spectral data measured over a range of temperatures are reported for copper(I) binding to aqueous solutions of rabbit liver zinc metallothionein at pH 7. These data provide a unique probe of the pathways adopted as copper–thiolate clusters form in the metallothionein. Metal analysis shows that, at low temperatures (<15 °C), Cu(I) displaces the Zn(II) linearly as a function of [Cu(I)] until 12 Cu(I) have been added, at which point all 7 Zn(II) are displaced. At high temperatures, significant hysteresis in the displacement of the Zn(II) results in nonlinearity in the [Zn(II)] vs [Cu(I)] line at the 6 Cu(I) point. As Cu(I) is added to Zn<sub>7</sub>-MT an emission band near 600 nm intensifies at all temperatures. At low temperatures (0 °C < T < 15 °C) the normalized intensity (emission intensity as a function of Cu(I) bound) increases roughly linearly with a significant increase in emission when 12 Cu(I) are bound. At higher temperatures (15 °C < T < 50 °C) a completely different relationship between emission intensity and molar ratio of Cu(I) added to the Zn<sub>7</sub>-MT is observed. The normalized emission intensity *decreases* between 2 and 7 Cu(I) added. Between 7 and 12 Cu(I) added there is a dramatic increase in emission intensity. As at low temperatures, the emission intensity for 12 Cu(I) greatly exceeds 12 times the intensity for 1 Cu(I). The emission intensity decreases toward zero as from 13 to 20 Cu(I) are added at all temperatures. The band center of the copper–thiolate emission near 600 nm remains approximately constant until 11 Cu(I) have been added and then blue shifts sharply at the 12 Cu(I) point, before significantly red shifting by 20 nm between 13 and 16 Cu(I). The emission intensity changes dramatically following temperature cycles between low and high temperatures. These changes can only be interpreted in terms of the mobility of the Cu(I) bound to the protein. When between 1 and 7 Cu(I) are added to Zn<sub>7</sub>-MT at 6 °C, the emission intensity is relatively high. Upon heating to 50 °C, the emission intensity drops to 10% of this initial value and cooling the solution back to 6 °C only recovers 40% of the original intensity. In complete contrast, for solutions containing between 8 and 12 Cu(I), the intensity after this same cycle is twice that of the original solution. The emission intensity clearly probes the location and structural features of the copper–thiolate clusters that form as up to 12 Cu(I) bind to the 20 cysteinyl thiols in metallothionein. *Through interpretation of these experimental properties, the pathways by which individual Cu(I) atoms bind to Zn<sub>7</sub>-MT can be completely described on the basis of the following:* (i) Cu(I) thiolate clusters in the  $\alpha$  domain emit 4–10 times the light of Cu(I) in the  $\beta$  domain. (ii) Cu(I) atoms located in the  $\alpha$  domain can be detected by this high emission intensity. (iii) Cu(I) binds in a distributed manner statistically across both domains at all temperatures. (iv) At high temperatures Cu(I) redistributes to populate the  $\beta$  domain, forming the domain specific product, Cu<sub>6</sub>(S<sub>cys</sub>)<sub>9</sub>- $\beta$ , which results in significant reduction in the emission intensity. (v) Cu(I) does not bind to Zn<sub>7</sub>-MT cooperatively. (vi) Cu<sub>12</sub>-MT is a tight structure, efficiently excluding solvent access to the Cu(I)–thiolate clusters. Finally, (vii) analysis of changes in the emission intensities as a function of temperature shows that these data provide a unique and sensitive probe of solvent access to the metal–thiolate clusters through the outer structure of the metal binding site. Analysis of the emission quenching suggests that the crevices predicted in the structure of Cu<sub>12</sub>-MT by molecular modeling techniques are present in Cu<sub>12</sub>-MT much like in the structure of Cd<sub>5</sub>Zn<sub>7</sub>-MT.

## Introduction

Copper is the third most abundant metallic element in the body (following iron and zinc).<sup>1,2</sup> It plays an important role in many biological functions, and abnormal copper metabolism can lead to Wilson's or Menkes' diseases in human beings.<sup>3</sup> A number of metalloproteins which contain copper have been identified, including cytochrome oxidase, the copper blue proteins, hemocyanins, and superoxide dismutase. These proteins function either in redox roles or as oxygen carriers, and hence, the bound copper can be either in the +1 or the +2 oxidation state. A single copper ion may be bound in a distorted tetrahedral (the one-copper blue proteins) or square-planar environment (superoxide dismutase), two copper ions may be bound in close proximity (hemocyanins), or many copper ions may be bound in a combination of the above

binding sites (laccase, ceruloplasmin, ascorbate oxidase, and cytochrome oxidase).<sup>4</sup> Despite the large number of copper ions present in the oxidases and blue copper proteins, there is no evidence for cluster formation involving either metal–metal binding or L–M–L–M–L units, where L is a bridging ligand. The characterization of the iron–sulfur proteins involving both inorganic sulfur and cysteinyl sulfur confirmed metal–sulfur cluster formation as a common structural motif in metalloproteins. More recently, metal–cysteinyl thiolate cluster formation has been demonstrated for the mammalian cadmium and zinc metallothioneins, Cd<sub>7</sub>-MT and Zn<sub>7</sub>-MT, and for copper- and silver-substituted yeast metallothioneins.<sup>5</sup>

Metallothioneins have been found in almost all mammals, as well as in fish, birds, invertebrates, and microorganisms. Many physiological roles have been proposed for these proteins, including transport, storage, and detoxification of a number of essential and nonessential trace metals.<sup>6–8</sup> The sequences of these proteins vary between species, but any polypeptide chain which has several

\* To whom correspondence should be addressed.

<sup>†</sup> Present address: Department of Chemistry, University of Virginia, Charlottesville, VA 22901.

Abstract published in *Advance ACS Abstracts*, July 1, 1994.

- (1) Underwood, E. J. *Trace Elements in Human and Animal Nutrition*, 4th ed.; Academic Press: New York, 1977.
- (2) Fitzgerald, F. *West. J. Med.* 1978, 128, 223–227.
- (3) Harris, E. D. In *Trace Elements in Health*; Rose, J., Ed.; Butterworths: Toronto, 1983; pp 44–73.

- (4) Cass, A. E. G.; Hill, H. A. O. In *Biological roles of Copper*; Ciba Foundation Symposium 79; Excerpta Medica: Amsterdam, 1980; pp 71–91.

- (5) Narula, S. S.; Winge, D. R.; Armitage, I. M. *Biochemistry* 1993, 32, 6773–6787.

of the following features can be designated a metallothionein (MT): (i) a low molecular weight, (ii) a high metal content, (iii) a characteristic amino acid composition which features a high content of cysteinyl residues but no aromatic amino acids or histidine residues, (iv) a unique amino acid sequence which shows a fixed distribution of cysteinyl residues, and (v) optical features characteristic of metal–thiolate bonds.<sup>9</sup> The structures of mammalian cadmium- and zinc-containing metallothioneins have been well established using the techniques of <sup>113</sup>Cd NMR,<sup>10</sup> 2D <sup>1</sup>H NMR,<sup>11</sup> and X-ray crystallography.<sup>12,13</sup> Seven M(II) ions bind tetrahedrally to 20 cysteinyl residues in two metal–thiolate clusters of the form M<sub>4</sub>(S<sub>cys</sub>)<sub>11</sub> (the α domain) and M<sub>3</sub>(S<sub>cys</sub>)<sub>9</sub> (the β domain), where M = Cd(II), Zn(II), and Hg(II).

The first metallothionein to be isolated which contained exclusively copper was found in copper-supplemented yeast cells.<sup>14,15</sup> Cu-MT is also found naturally in mammalian fetal and neonatal liver tissue.<sup>16</sup> The formation of Cu-MT may also be induced by the injection of copper(II) salts.<sup>17–19</sup> Cu-MT may also be formed *in vitro* by using Cu(I) to displace the bound metals.<sup>20</sup> Little is known about the structure of mammalian copper-containing metallothioneins. The coordination number and geometry of the copper in copper–metallothioneins have not been established in general. EXAFS studies have suggested several possibilities: (i) solely tetrahedral copper (in yeast Cu-MT),<sup>21,22</sup> (ii) solely trigonal copper (in mammalian and yeast Cu-MT),<sup>23–25</sup> and (iii) a mixture of both digonal and trigonal coppers (in yeast Cu-MT).<sup>26</sup> A single cluster structure, Cu<sub>7</sub>(S<sub>cys</sub>)<sub>10</sub>, involving both digonal and trigonal coordination of the copper in yeast Cu-MT has been proposed on the basis of the 2D <sup>1</sup>H NMR similarities between copper- and silver-substituted yeast MT and silver–thiolate connectivities suggested by HMQC NMR studies on the silver-substituted protein.<sup>5</sup>

Before precise structural data can be determined, metal to protein stoichiometric ratios that result in the formation of complexes that adopt specific three-dimensional structures must be established. Optical spectroscopy can provide extremely precise

metal to protein stoichiometric ratios from dilute aqueous solutions at neutral pH. Since copper bound to metallothionein is found exclusively in the +1 oxidation state, spectroscopic techniques available for monitoring metal binding in metallothioneins are limited. Unlike complexes containing the d<sup>9</sup> Cu(II) ion, Cu(I) compounds (with a filled 3d<sup>10</sup> shell) are diamagnetic and are generally colorless due to a lack of intrametallic d–d transitions. This eliminates the use of spectroscopic techniques traditionally used to study Cu(II) proteins such as: electron paramagnetic resonance (EPR) spectroscopy,<sup>27</sup> electron–nuclear double resonance (ENDOR) spectroscopy,<sup>28</sup> and even UV–visible absorption spectroscopy.<sup>27,29,30</sup> Our group has previously used circular dichroism spectroscopy (CD), magnetic circular dichroism spectroscopy (MCD), and luminescence spectroscopy to directly monitor metal binding between d<sup>10</sup> metals and metallothionein.<sup>31–42</sup> The spectral saturation points of these techniques at specific stoichiometric ratios of metal to protein coincide with the formation of known structures for CD<sub>7</sub>-MT and suggest specific complexes form for Ag<sub>12</sub>-MT, Ag<sub>18</sub>-MT, Hg<sub>7</sub>-MT, and Hg<sub>18</sub>-MT.

In this paper, we report detailed emission spectroscopic data over a range of conditions that show with fine detail the formation of the copper–thiolate cluster structure in rabbit liver metallothionein Cu<sub>n</sub>-MT (*n* = 1–20). Excited-state properties are sensitive to many energy dissipation processes, the most significant of which in solution is solvent deactivation. The exposure of the metals in the binding sites to solvent molecules can be probed using changes in the emission properties as a function of temperature and metal loading. Our data suggest that a Cu<sub>12</sub>-MT species forms which consists of a core of copper–thiolate clusters which are well protected from the solvent by the protein backbone. We report that Cu(I) binds to Zn<sub>7</sub>-MT 2 in a distributed manner under all tested conditions followed by rearrangement to the domain specific product at elevated temperatures. We also describe how a proposed structure for the Cu<sub>12</sub>-MT clusters based on molecular modeling techniques<sup>64</sup> accounts for the observed emission data. We conclude from the emission data that crevices first reported in the structure of Cd<sub>5</sub>-Zn<sub>2</sub>-MT by Stout<sup>12,13</sup> also must exist in the outer peptide-based structure that surrounds the metal binding site in Cu<sub>12</sub>-MT.

## Experimental Section

Zn<sub>7</sub>-MT was isolated from rabbit livers following *in vivo* induction procedures using aqueous zinc salts. The protein was purified using gel

- (6) *Metallothionein I*; Kagi, J. H. R., Nordberg, M., Eds.; Birkhauser Verlag: Basel, Switzerland, 1979.
- (7) *Metallothionein II*; Kagi, J. H. R.; Kojima, Y., Eds.; Birkhauser Verlag: Basel, Switzerland, 1987; Exp. Suppl. 52.
- (8) Hunziker, P. E.; Kagi, J. H. R. In *Metalloproteins-Part II: Metal Proteins with Non-Redox Roles*; Harrison, P. M., Ed.; The MacMillan Press Ltd.: London, 1985; pp 149–182.
- (9) Nordberg, M.; Kojima, Y. In *Metallothionein I*; Kagi, J. H. R., Nordberg, M., Eds.; Birkhauser Verlag: Basel, Switzerland, 1979; pp 41–116.
- (10) Otvos, J. D.; Armitage, I. M. *Proc. Natl. Acad. Sci. U.S.A.* **1980**, *77*, 7094–7098.
- (11) Messerle, B. A.; Schaffer, A.; Vasak, M.; Kagi, J. H. R.; Wurthrich, K. *J. Mol. Biol.* **1992**, *225*, 433–443.
- (12) Robbins, A. H.; McRee, D. E.; Williamson, M.; Collett, S. A.; Xuong, N. H.; Furey, W. F.; Wang, B. C.; Stout, C. D. *J. Mol. Biol.* **1991**, *221*, 1269–1293.
- (13) Robbins, A. H.; Stout, C. D. In *Metallothioneins*; Stillman, M. J., Shaw, C. F., III, Suzuki, K. T., Eds.; VCH Publishers: New York, 1992; pp 31–54.
- (14) Prinz, R.; Weser, U. *Hoppe-Seyler's Z. Physiol. Chem.* **1975**, *356*, 767–776.
- (15) Prinz, R.; Weser, U. *FEBS Lett.* **1975**, *54*, 224–229.
- (16) Hartmann, H.; Weser, U. *Biochim. Biophys. Acta* **1977**, *491*, 211–222.
- (17) Premakumar, R.; Winge, D. R.; Wiley, R. D.; Rajagopalan, K. V. *Arch. Biochem. Biophys.* **1975**, *170*, 267–277.
- (18) Bremner, I.; Young, B. W. *Biochem. J.* **1976**, *157*, 517–520.
- (19) Bremner, I. *J. Nutr.* **1987**, *117*, 19–29.
- (20) Nielson, K. B.; Atkin, C. L.; Winge, D. R. *J. Biol. Chem.* **1985**, *260*, 5342–5350.
- (21) Bordas, J.; Koch, M. H. J.; Hartmann, H.-J.; Weser, U. *FEBS Lett.* **1982**, *140*, 19–21.
- (22) Freedman, J. H.; Posers, L.; Peisach, J. *Biochemistry* **1986**, *25*, 2342–2349.
- (23) George, G. N.; Winge, D.; Stout, C. D.; Cramer, S. P. *J. Inorg. Biochem.* **1986**, *27*, 213–220.
- (24) Abrahams, I. L.; Bremner, I.; Diakun, G. P.; Garner, C. D.; Hasnain, S. S.; Ross, I.; Vasak, M. *Biochem. J.* **1986**, *236*, 585–589.
- (25) George, G. N.; Byrd, J.; Winge, D. R. *J. Biol. Chem.* **1988**, *263*, 8199–8203.
- (26) Pickering, I. J.; George, G. N.; Dameron, C. T.; Kurz, B.; Winge, D. R.; Dance, I. G. *J. Am. Chem. Soc.* **1993**, *115*, 9498–9505.

- (27) Malkin, R.; Malmstrom, B. G. *Adv. Enz.* **1970**, *33*, 177–244.
- (28) Roberts, J. E.; Cline, J. F.; Lum, V.; Freeman, H.; Gray, H. B.; Peisach, J.; Reinhammar, B.; Hoffman, B. M. *J. Am. Chem. Soc.* **1984**, *106*, 5324–5330.
- (29) Solomon, E. I.; Hare, J. W.; Dooley, D. M.; Dawson, J. H.; Stephens, P. J.; Gray, H. B. *J. Am. Chem. Soc.* **1980**, *102*, 168–178.
- (30) Solomon, E. I.; Hare, J. W.; Gray, H. B. *Proc. Natl. Acad. Sci. USA* **1976**, *73*, 1389–1393.
- (31) Stillman, M. J.; Zelazowski, A. J.; Szymanska, G.; Gasyina, Z. *Inorg. Chim. Acta* **1989**, *161*, 275–279.
- (32) Stillman, M. J.; Zelazowski, A. J.; Gasyina, Z. *FEBS Lett.* **1988**, *240*, 159–162.
- (33) Stillman, M. J.; Law, A. Y. C.; Cai, W.; Zelazowski, A. J. In *Metallothionein II*; Kagi, J. H. R., Kojima, Y., Eds.; Birkhauser Verlag: Basel, Switzerland, 1987; Exp. Suppl. 52, pp 203–211.
- (34) Zelazowski, A. J.; Gasyina, Z.; Stillman, M. J. *J. Biol. Chem.* **1989**, *264*, 17091–17099.
- (35) Gasyina, Z.; Zelazowski, A.; Green, A. R.; Ough, E.; Stillman, M. J. *Inorg. Chim. Acta* **1988**, *153*, 115–118.
- (36) Cai, W.; Stillman, M. J. *J. Am. Chem. Soc.* **1988**, *110*, 7872–7873.
- (37) Stillman, M. J.; Cai, W.; Zelazowski, A. J. *J. Biol. Chem.* **1987**, *262*, 4538–4548.
- (38) Stillman, M. J.; Zelazowski, A. J. *J. Biol. Chem.* **1988**, *263*, 6128–6133.
- (39) Zelazowski, A. J.; Stillman, M. J. *Inorg. Chim. Acta* **1992**, *31*, 3363–3370.
- (40) Stillman, M. J. In *Metallothioneins*; Stillman, M. J., Shaw, C. F., III, Suzuki, K. T., Eds.; VCH Publishers: New York, 1992; pp 55–127.
- (41) Lu, W.; Stillman, M. J. *J. Am. Chem. Soc.* **1993**, *115*, 3291–3299.
- (42) Lu, W.; Zelazowski, A. J.; Stillman, M. J. *Inorg. Chim. Acta* **1993**, *32*, 919–926.

filtration and electrophoresis as previously described.<sup>37,43</sup> Aqueous protein solutions were prepared by dissolving the protein in argon-saturated distilled water. Protein concentrations were estimated from measurements of the –SH group and zinc concentrations as described previously. These estimations were based on the assumption that there are 20 –SH groups and 7 Zn atoms in each protein molecule. The concentration of –SH groups was determined by the spectrophotometric measurement of the colored thionitrobenzoate anion ( $\epsilon_{420} = 13\,600\text{ M}^{-1}\text{ cm}^{-1}$ ) produced by reaction with DTNB (5,5'-dithiobis(2-nitrobenzoic acid)) in the presence of 6 M guanidine hydrochloride.<sup>44</sup> Zinc concentrations were determined by flame atomic absorption spectroscopy (AAS) using a Varian AA875 atomic absorption spectrophotometer with a Varian Model 55 programmable sampler changer.

Solutions of 10  $\mu\text{M}$  aqueous Zn<sub>7</sub>-MT were titrated with Cu(I) in the form of  $[\text{Cu}(\text{CH}_3\text{CN})_4]\text{ClO}_4$ . This salt was prepared by the method of Hemmerich and Sigwart<sup>45</sup> and was dissolved in a 30% (v/v) acetonitrile/water solution. Unless stated otherwise, protein solutions were bubbled with Ar for 5 min after each addition of Cu(I) before measuring spectral data.

Metal displacement studies were carried out using basic Chelex-100 resin as a chelating agent for the free metals in solution.<sup>46</sup> Cu(I) was added in mole equivalents (1 mol of Cu(I)/mol of protein) aliquots to individual 2-mL samples of 10  $\mu\text{M}$  Zn-MT 2 equilibrated at a given temperature. Each sample was bubbled with Ar for 5 min between each addition. After the Cu(I) had been added, the emission spectrum was recorded and the solution was mixed with ~65 mg of Chelex-100 resin for 5 min at the equilibrium temperature. The metal concentrations of the supernatant (which represented the metals still bound to MT) were determined by AAS.

Emission spectra were measured on a Photon Technology Inc. LS-100 spectrometer. The temperature of the titrations was controlled using an Endocirculating bath to pump a 50% ethylene glycol/water mixture around the cell compartment. Optical glass filters were placed over the excitation (Corning 7-54 or Schott BG-24) and emission slits (Corning CS 3-74 or Schott GG-420) for observation of emission in the 500–700-nm region with excitation at 300 nm. The emission spectral data were processed using the programs Spectra Manager<sup>47</sup> and Plot3D<sup>48</sup> and replotted on an HP 7550A plotter.

## Results

**Copper Binding to Zn<sub>7</sub>-MT.** Metallothionein binds copper only in the +1 oxidation state. Cu(II) reacts with metallothionein to form Cu(I) and probably denatures the protein through oxidation of the cysteinyl thiolates.<sup>49</sup> In this present study, aliquots of the Cu(I) salt  $[\text{Cu}(\text{CH}_3\text{CN})_4]\text{ClO}_4$  were added to aqueous Zn<sub>7</sub>-MT 2 to replace the tetrahedrally-bound Zn(II) between 7 and 50 °C.

Figure 1 shows the number of Zn(II) ions remaining bound to metallothionein at various stages of copper loading over the range of temperatures used for the emission titrations described later. Data from experiments carried out at the temperature extremes of 7 and 50 °C are shown. (Data for 22 °C, not shown, follow the data for 7 °C.) Increasing amounts of Cu(I) were added to individual solutions of Zn-MT 2 and the metal concentrations measured by AAS using basic-pH Chelex-100 resin to sequester the free metal ions in solution. Chelex-100 resin is an effective chelator of metals over the temperature range –20 to 65 °C, and the resin does not remove zinc directly from the metallothionein binding sites within the time scale of these experiments.<sup>46</sup> Analysis of the Cu concentrations (not shown) shows that none of the Cu(I) is free in solution up to the addition of 12 Cu(I) (i.e. all Cu(I) (up to 12 mol equiv) bind to the protein within 5 min).

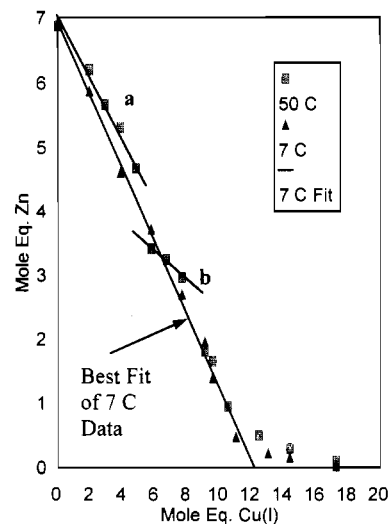


**Figure 1.** Mole equivalents of Zn(II) bound to MT 2 as Cu(I) is added. Cu(I) was added to separate solutions of Zn-MT 2 at the stated temperature, and Chelex-100 was used to remove the free metal ions before determining the Zn concentration by AAS. Individual points represent the average of five measurements on each of two solutions. The error associated with these measurements is approximately 0.1 mol equiv of Zn(II). This error is approximately equivalent to the size of the symbols used on the graph. The heavy line represents the best fit straight line for the data between 0 and 12 mole equiv of Cu(I) at 7 °C (triangles). The shorter lines (labeled a and b) represent regions of deviation from a stoichiometric displacement of Zn(II) by the Cu(I) at 50 °C (squares).

Although the analytical data appear to show that Cu(I) displaces Zn(II) on a charge basis at each temperature, in fact there are several trends revealed in this plot. If the displacement occurred strictly on a charge compensation basis, it would take 14 Cu(I) [14(+1)] to displace all of the Zn(II) [7(+2)]. In fact, the Zn(II) is displaced at the 12 Cu(I) point at all temperatures. Similar results were obtained during addition of Cu(I) to rat liver Cd, Zn-MT using dialysis as the technique to remove free ions (i.e. at 12 Cu(I) added, all Zn(II) and Cu(II) had been displaced).<sup>50</sup> Second, Zn(II) is displaced differently at the two temperatures. At 50 °C, Zn(II) displacement lags during the addition of the first 5 Cu(I) (a). A sharp loss of Zn(II) from 4.5 to 3.5 is associated with the addition of the 6th Cu(I) to the protein. Zn(II) displacement again lags between 6 and 8 Cu(I) (b), and hysteresis in the Zn concentration as a function of Cu(I) added is clearly observed between the addition of the 8th and 9th Cu(I).

### Dependence of the Emission Intensity on the Cu(I) to MT Ratio.

Figures 2–6 show the temperature dependence of the emission spectrum of Cu-MT as a function of copper loading. The emission data were measured from aqueous solutions of rabbit liver Zn<sub>7</sub>-MT 2 held at the stated temperature (10, 23, and 40 °C) at pH 6.6. The third axis in Figures 2–4 represents the moles of Cu(I) added per mole of protein (mole equiv), and the lower plane shows a contour diagram of the surface, similar to a geographical contour map. When the sample is excited at 300 nm, the presence of copper in metallothionein gives rise to an emission maximum near 600 nm.<sup>51</sup> Previously-reported data recorded on a Perkin-Elmer MPF4 spectrofluorometer exhibit two overlapping bands,<sup>35</sup> however the data obtained using the greater sensitivity of the LS-100 instrument with a red-sensitive phototube shows that the band is actually homogeneous, with only one maximum (and minimal emission intensity between 700 and 800 nm).

Figure 2 shows the emission data obtained when Cu(I) is added in microliter aliquots to a single aqueous solution of Zn<sub>7</sub>-MT

(43) Zelazowski, A. J.; Szymanska, J. A.; Witas, H. *Prep. Biochem.* **1980**, *10*, 495–505.

(44) (a) Ellman, G. L. *Arch. Biochem. Biophys.* **1959**, *82*, 70–77. (b) Birchmeier, W.; Christen, P. *FEBS Lett.* **1971**, *18*, 209–213.

(45) Hemmerich, P.; Sigwart, C. *Experientia* **1963**, *19*, 488–489.

(46) Cai, W.; Stillman, J. M. *Inorg. Chim. Acta* **1988**, *152*, 111–115.

(47) Browett, W. R.; Stillman, M. J. *Comput. Chem.* **1987**, *11*, 73–80.

(48) Gasyana, Z.; Stillman, M. J. Unpublished program.

(49) (a) Suzuki, K. T.; Maitani, T. *Biochem. J.* **1981**, *199*, 289–295. (b) Nielson, K. B.; Winge, D. R. *J. Biol. Chem.* **1984**, *259*, 4941–4946.

(50) Law, A. Y. C. *Ph.D. Thesis*; University of Western Ontario, London, Ontario, 1984.

(51) Stillman, M. J.; Gasyana, Z. In *Methods in Enzymology, Volume 205, Metallobiochemistry Part B*; Riordan, J. F., Vallee, B. L., Eds.; Academic Press: Orlando, FL, 1991; pp 540–555.

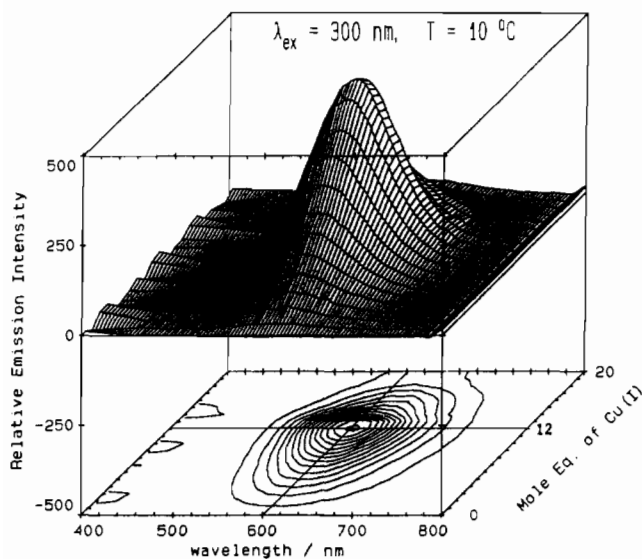


**Figure 2.** Three-dimensional plot showing changes in emission spectra as a function of the Cu(I):MT molar ratio for a single solution of rabbit liver Zn-MT 2 at 10 °C and pH 6.6 following excitation at 300 nm. The third axis represents the moles of Cu(I) added per mole of protein (mole equiv), and the lower plane shows a contour diagram of the surface (taking 30 vertical cuts), similar to a geographical contour map. The grid line drawn across the contour diagram represents a Cu(I) molar ratio of 12, and the grid line parallel to the z-axis represents the 600-nm point in the spectra. Note that the contour diagram shows a *gradual increase* in emission intensity for  $\text{Cu}_0\text{Zn}_7\text{-MT}$  to  $\text{Cu}_{12}\text{-MT}$ .

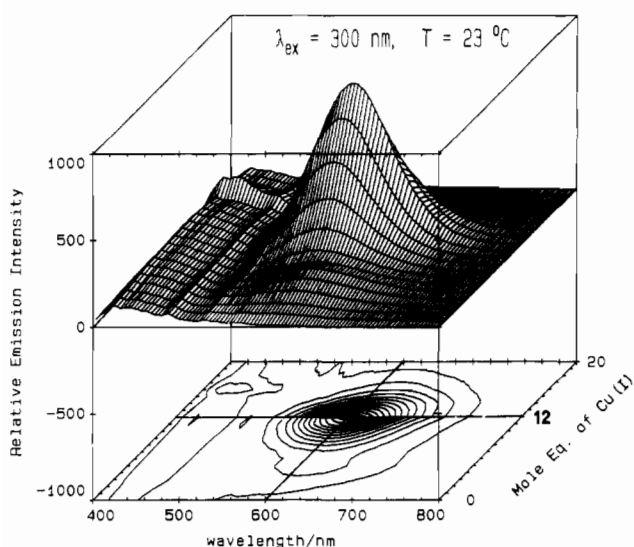


**Figure 3.** Three-dimensional plot showing changes in emission spectra as a function of the Cu(I):MT molar ratio for a single solution of rabbit liver Zn-MT 2 at 23 °C and pH 6.6 following excitation at 300 nm. The grid line drawn across the contour diagram represents a Cu(I) molar ratio of 12, and the grid line parallel to the z-axis represents the 600-nm point in the spectra. Note that the contour diagram shows that the change in emission intensity for  $\text{Cu}_0\text{Zn}_7\text{-MT}$  to  $\text{Cu}_6\text{Zn}_4\text{-MT}$  is much less than that between  $\text{Cu}_6\text{Zn}_4\text{-MT}$  and  $\text{Cu}_{12}\text{-MT}$ .

equilibrated at 10 °C. The contour plot shows clearly that the intensity grows symmetrically around a 600-nm band center to reach a maximum at 12 Cu(I). A red shift of the band center occurs as the emission intensity diminishes past 12 Cu(I). Figure 5A shows the normalized emission intensity at the band maximum (approximately 600 nm) as a function of the Cu(I):MT ratio for the data in Figure 5A are on a per Cu(I) basis. Therefore, an increase means that proportionally greater intensity is observed. At 10 °C, the quantum yield of emission per Cu(I) increases almost linearly from the first addition of Cu(I) up to the 12th addition and then decreases steeply. Figure 6A shows the wavelength

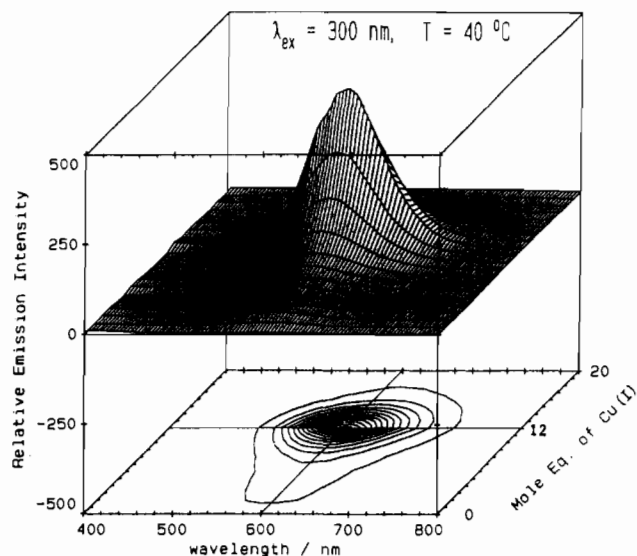


**Figure 4.** Three-dimensional plot showing changes in emission spectra as a function of the Cu(I):MT molar ratio for a single solution of Zn-MT 2 at 40 °C and pH 6.6 following excitation at 300 nm. The grid line drawn across the contour diagram represents a Cu(I) molar ratio of 12, and the grid line parallel to the z-axis represents the 600-nm point in the spectra. Note that the contour diagram shows *no change* in intensity between  $\text{Cu}_2\text{Zn}_6\text{-MT}$  and  $\text{Cu}_6\text{Zn}_4\text{-MT}$ .

dependence of the center of the emission band maximum at 10 °C on the degree of copper loading. From 1–10 Cu(I), the band center remains close to 603 nm. A major red shift to 623 nm occurs between 12 and 18 Cu(I).

Figure 3 shows the dependence of the emission spectrum on Cu(I) loading at 23 °C. We see a significantly different pattern. Although the 600-nm band grows in intensity, with the same dramatic increase in emissive yield per Cu(I) at 12 Cu(I) (Figure 5B) as seen at 10 °C (Figure 5A), the intensity at 23 °C in the early part of the titration, from 1–7 Cu(I), does not increase linearly. As is clear in Figure 3 and emphasized in the normalized plot in Figure 5B, there is very little intensity change until 8 Cu(I) have been added. In fact the normalized intensity decreases from 3 Cu(I) to 6 Cu(I) (Figure 5B). In addition to changes in intensity, the band maximum near 600 nm also exhibits a strong dependence on the Cu(I) loading. Figure 6B shows that the band maximum remains constant within experimental error at 601 nm from 1 Cu(I) to 10 Cu(I). A blue shift to 598 nm between 11 and 12 Cu(I) is followed by a steep red shift to 622.5 nm at 16 Cu(I) before relaxing to 618 nm at 20 Cu(I).

Figures 4 and 5C show that the trend in the reduction in the normalized emission intensities from 2 to 6 Cu(I) between 10 and 23 °C continues at 40 °C. The emission intensity now increases only for copper loadings above 6 Cu(I):MT. It is important to note that it would be expected that the copper-dependent emission would intensify by up to 6-fold as the Cu(I):MT ratio increases from 1 to 6; therefore this *lack* of intensification must directly probe differences in the structure of the Cu(I) binding site. Since there is little change in emission intensity between the 2nd and 6th additions of Cu(I), the quantum yield per Cu(I) actually decreases for this region of the titration (Figure 5C). This normalized intensity plot emphasizes even more strongly how formation of the  $\text{Cu}_{12}(\text{S}_{\text{cys}})_{20}\text{-MT}$  species results in a maximum in the emissive intensity. The values near 20 Cu(I) show that there is a very low emission intensity for  $\text{Cu}_{20}\text{-MT}$ . As at the other two reported temperatures (10 and 23 °C), the center of the band maximum is directly dependent on the degree of copper loading (Figure 6C). The 40 °C data show that there is an overall blue shift in each band center as the temperature increases.

The  $\text{Cu}_{12}\text{-MT}$  species (as indicated by the maximum in emission intensity) can be regenerated when stoichiometric amounts of  $\text{Zn}_7\text{-MT}$  are added to the  $\text{Cu}_{20}\text{-MT}$  species (low emission

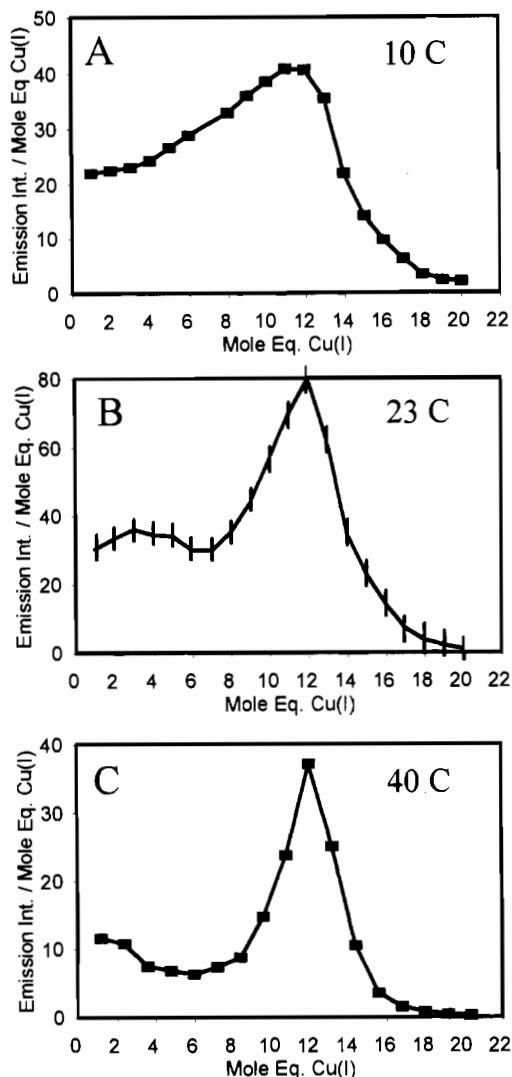


**Figure 5.** Normalized emission intensity (intensity at 600 nm divided by the number of mole equiv of Cu(I) present) vs mole equiv Cu(I) added at (A) 10 °C, (B) 23 °C, and (C) 40 °C. The data in Figure 5B represent the average of two titrations with the bars showing the approximate error at each point in the titration. If there was no change in the quantum yield per copper, this graph would yield a horizontal line.

intensity). This is evident by the re-formation of both the CD and emission spectrum. This reversibility indicates the *no oxidation* of the protein occurs in the aqueous environment when greater than 12 Cu(I) are present.

**Effect of Equilibration Temperature and Time on Emission Intensity.** Although the shape of the three-dimensional surface of emission intensity ( $y$ ) as a function of wavelength ( $x$ ) and of Cu:MT mole ratio ( $z$ ) is significantly temperature dependent (Figures 2–4), no significant changes are observed in the absorption spectra at 300 nm for titrations carried out at 5 and 46 °C. Changes in the absorption spectra do not provide an explanation for the great differences in emission spectral intensities. Clearly, changes in the emission intensity must be due to the temperature dependence of copper–thiolate cluster formation and, in particular, the location of individual Cu(I) within the two domains. In previous studies of Cd(II) binding to Zn<sub>7</sub>-MT, we observed that the Cd(II) are quite mobile at high temperatures when bound to MT.<sup>37,38</sup> In Figures 7–10, we show how the mobility of the Cu(I) influences the emission intensity at 600 nm.

Solutions of Zn<sub>7</sub>-MT containing varying amounts of Cu(I) were subjected to several temperature cycles to investigate the conditions for forming the thermodynamically preferred metal–thiolate cluster product. The final emission spectrum of solutions containing <8 Cu(I) that were made at 6 °C, heated to 50 °C,

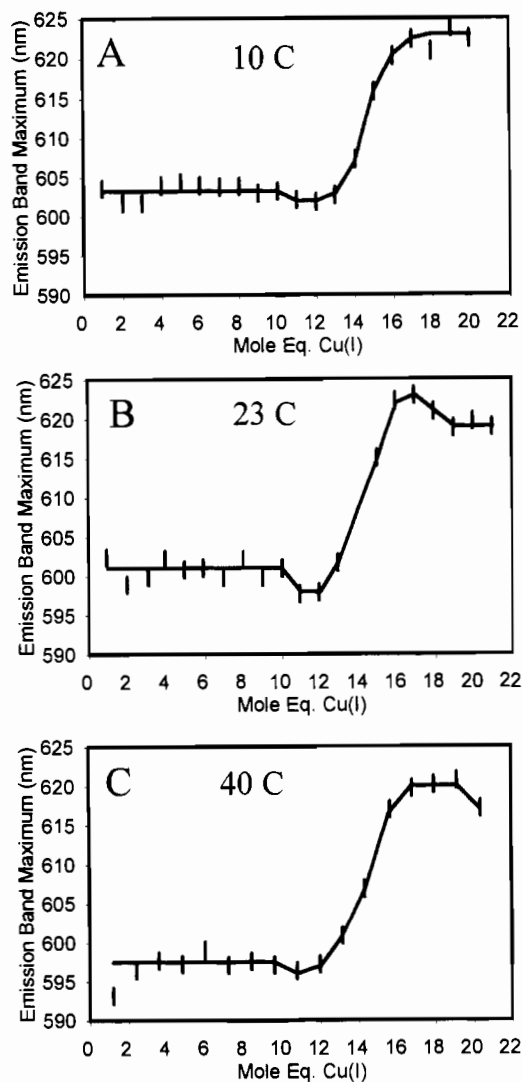


**Figure 6.**  $\lambda_{em}$  vs mole equiv of Cu(I) added at (A) 10 °C, (B) 23 °C, and (C) 40 °C. The markers represent the error associated with determining the band center at half-height. In (A), the mean value of  $\lambda_{em}$  between 1 and 10 Cu(I) is 603 nm and  $\lambda_{em}$  drops to a minimum at 602 nm at Cu<sub>12</sub>-MT and then rises rapidly to a maximum at 623 nm at Cu<sub>16</sub>-MT. In (B), the mean value of  $\lambda_{em}$  between 1 and 10 Cu(I) is 601 nm and  $\lambda_{em}$  drops to a minimum at 598 nm at Cu<sub>12</sub>-MT and then rises rapidly to a maximum at 623 nm at Cu<sub>16</sub>-MT. The band maximum then blue shifts slightly to 619 nm when >16 Cu(I) have been added. In Figure (C), the mean value of  $\lambda_{em}$  between 1 and 10 Cu(I) is 597.5 nm.  $\lambda_{em}$  drops to a minimum at 596 nm at Cu<sub>12</sub>-MT before rising rapidly to a maximum at 620 nm at Cu<sub>16</sub>-MT. The band maximum then blue shifts slightly to 617 nm when >16 Cu(I) have been added.

and then cooled back down to 6 °C exhibited a lower intensity than the initial intensity at 6 °C. (The emission intensity dropped to about 40% of the original in the case of Zn-MT + 6 Cu(I); Figure 7). In complete contrast, solutions containing between 8 and 12 Cu(I) treated similarly showed a much greater final emission intensity after the temperature cycle. (The intensity almost doubles in the case of Zn-MT + 12 Cu(I); Figure 8). Note that the shape of the emission envelope remains the same at all three temperatures. Further temperature cycles did not affect the intensity of the spectra measured at 6 °C for any of the samples.

Figure 9A–C shows how the emission intensity changes as solutions of Zn<sub>7</sub>-MT with 6, 9, and 12 Cu(I), respectively, are cooled from 50 °C. The aliquots of Cu(I) were added at 50 °C, each solution was equilibrated at the set temperature, and the emission spectrum was measured. As expected from Figures 7 and 8, solutions made near 50 °C emit more strongly when cooled to 6 °C (direction a to b, in Figure 9A–C). The increase in

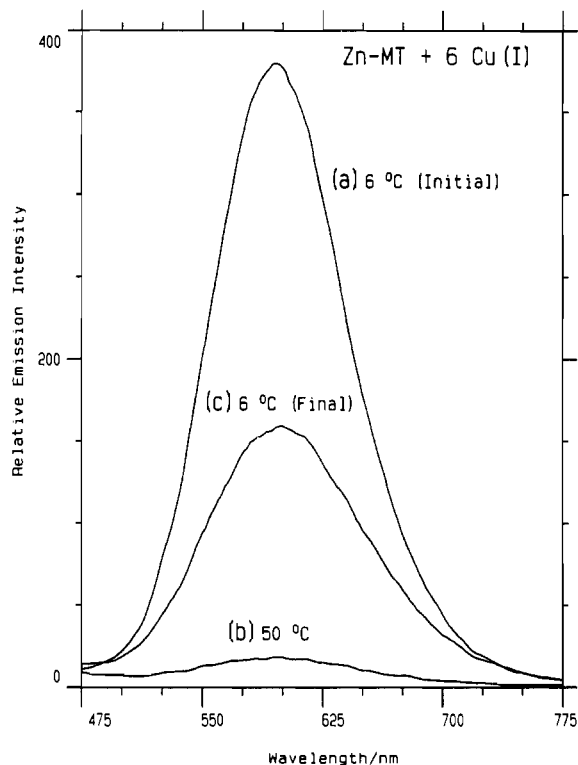


**Figure 7.** Emission spectrum of Zn-MT 2 + 6 Cu(I) after a single warm-cool cycle. The initial spectrum (a) was recorded after 6 mole equiv of Cu(I) had been added to a solution of Zn-MT 2 at 6 °C. The solution was then heated to 50 °C (b) and then cooled back to 6 °C (c). The data represent typical results obtained when 1–7 Cu(I) are added to Zn<sub>7</sub>-MT.

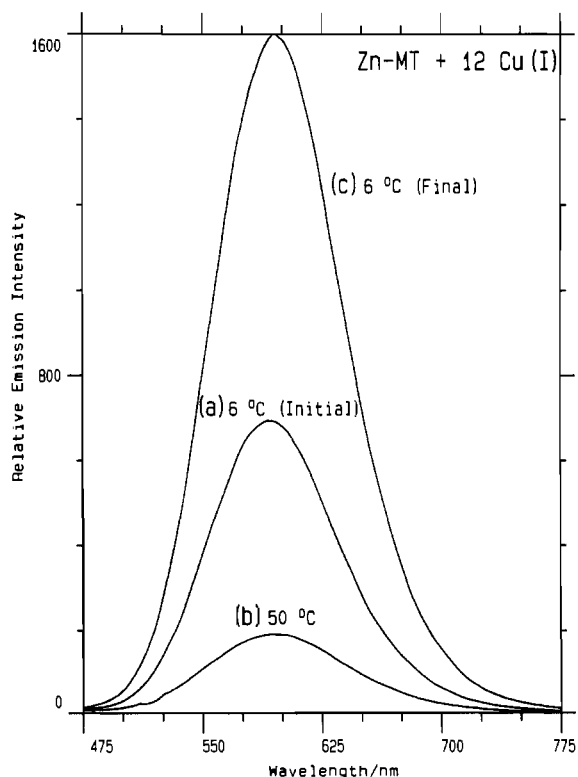


**Figure 8.** Emission spectrum of Zn-MT 2 + 12 Cu(I) after a single warm-cool cycle. The initial spectrum (a) was recorded after 12 mole equiv of Cu(I) had been added to a solution of Zn-MT 2 at 6 °C. The solution was then heated to 50 °C (b) and then cooled back to 6 °C (c). In (c), the data represent typical results obtained when 8–12 Cu(I) are added to Zn<sub>7</sub>-MT.

intensity as the solution is cooled from 48 °C is clearly biphasic. In each case, the slope of the line describing the emission intensity

as a function of temperature is much less steep above 30 °C. Below 30 °C, there is a steep increase in emission intensity as the temperature is lowered.

In addition to the temperature dependence described above, the intensity of the emission is also dependent on time. The data plotted in Figure 10 compare the emission intensities at 600 nm of solutions of Cu<sub>n</sub>-MT ( $n = 1$ –20) prepared in three different ways: (a) Cu(I) was added to Zn<sub>7</sub>-MT at 19 °C, followed by 25 min of equilibration before the emission spectrum was measured. (b) Similar conditions were used, except that a 5-min equilibration period was used. (c) Cu(I) was added at 40 °C followed by equilibration for 5 min. The acquisition time for each emission spectrum is approximately 5 min; therefore, Figure 10 shows emission intensities from spectra recorded (a) at 20 °C with 30 min between each addition of Cu(I) (with 12 additions the elapsed time was 6 h), (b) at 20 °C with 10 min between each addition of Cu(I) (with 17 additions the elapsed time was approximately 3 h), and (c) at 40 °C with 10 min between additions (with 17 additions the elapsed time was approximately 3 h). The data have been normalized so that the maximum of the spectrum of Cu<sub>12</sub>-MT at 600 nm has the same intensity in each titration; however, there is no physical justification for doing so (see Figure 9C). This procedure emphasizes changes in relative intensities observed for each temperature and equilibration condition for the separate Cu<sub>n</sub>-MT species (with  $0 < n < 20$ ) formed during the titration. The trend in intensities as a function of the Cu(I):MT molar ratio emphasizes the rearrangement of Cu(I) to sites favored by a thermodynamic mechanism (long equilibration times (a), high temperatures (c)). Clearly, the thermodynamic product (illustrated by line c) results in lower relative emission intensity between 1 and 10 Cu(I).

**Solvent Effects.** Since the emission intensity of metal complexes is highly dependent on the accessibility of the emissive state to solvent molecules, changing the solvent can affect the luminescence if the solvent contributes significantly to radiationless transitions. In a binding site of the type proposed here for Cu<sub>12</sub>-MT (see below), larger solvent molecules may not be able to approach the luminophore as efficiently as smaller solvent molecules and, combined with differing vibrational energies of the solvent, quite large changes in quenching efficiencies may be observed. In addition to these general effects on the luminescent intensity, different solvents may significantly alter the binding properties of metallothionein with metals. This has been observed previously for copper binding to metallothionein in 25% acetonitrile<sup>52</sup> and with mercury binding to metallothionein in 50% ethylene glycol.<sup>41</sup> Solvent molecules (such as acetonitrile) may also compete with the protein molecule as ligands for Cu(I). In order to probe the solvent effects, titrations were carried out at room temperature in different solvent mixtures: (i) 50% (v/v) ethylene glycol/water; (ii) 50% (v/v) acetonitrile/water; (iii) 50% (v/v) deuterium oxide/water. In all cases, the center of the emission band (600 nm) reaches a maximum intensity with the formation of the Cu<sub>12</sub>-MT species and is more intense than if the titration had been carried out in water. In the case of acetonitrile and ethylene glycol, the reaction takes much longer to reach completion than it does in water.

## Discussion

During the isolation of Cu-MT from the ascomycete *Neurospora crassa*, Lerch and co-workers discovered an orange luminescence when fractions containing Cu-MT were illuminated with an ultraviolet lamp.<sup>53</sup> This emission was found to be dependent on the copper content of the protein and was attributed to the copper–thiolate chromophore.<sup>53</sup> Similar emission had been observed from powder complexes of Cu(I) with cysteine and with

(52) Li, Y.-J.; Weser, U. *Inorg. Chem.* **1992**, *31*, 5526–5533.

(53) Beltrami, M.; Lerch, K. *FEBS Lett.* **1981**, *127*, 201–203.

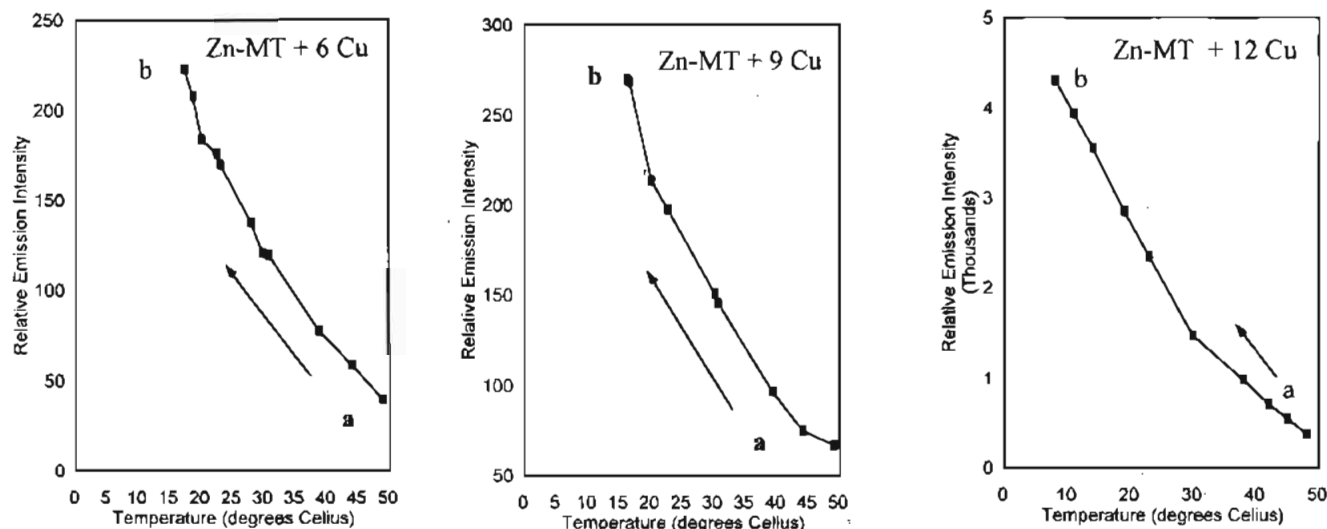


Figure 9. (A) Left; Emission intensity of the  $\text{Cu}_6\text{Zn}_4\text{-MT}$  species as a function of temperature. The data points are from a sample prepared at 48 °C and then cooled (a to b). (B) Middle; Emission intensity of the  $\text{Cu}_9\text{Zn}_7\text{-MT}$  species as a function of temperature. The data points are from a sample prepared at 48 °C and then cooled (a to b). (C) Right; Emission intensity of the  $\text{Cu}_{12}\text{-MT}$  species as a function of temperature. The data points are from a sample prepared at 48 °C and then cooled (a to b).

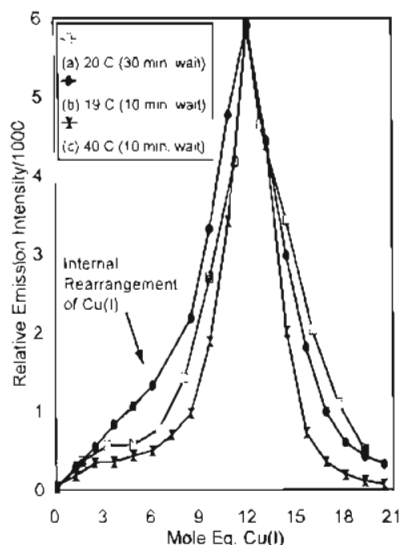


Figure 10. Relative emission intensity at 600 nm as a function of mole equiv of Cu(I) for solutions of  $\text{Zn}_7\text{-MT 2}$  titrated with Cu(I) (a) at 20 °C with 30 min between additions of Cu(I), (b) at 19 °C with 10 min between additions, and (c) at 40 °C with 10 min between additions. Each set of data points represents the emission intensity at 600 nm (or  $I_{\text{max}}$ ) as Cu(I) is sequentially added to a single solution of  $\text{Zn}_7\text{-MT 2}$  under the specified conditions. The data have been normalized at the intensity recorded  $\text{Cu}_{12}\text{-MT}$  species emission for easier comparison although there is no physical justification for doing so (see Figure 9C).

glutathione.<sup>54</sup> Luminescence spectra have since been reported from rat kidney Hg,Cu-MT<sup>55</sup> and Cd,Cu-MT,<sup>56</sup> fungal Cu-MT,<sup>57</sup> fetal bovine liver Cu,Zn-MT,<sup>58</sup> porcine liver Cu,Zn-MT<sup>59</sup> from Cu-binding peptides and mutants of yeast MT.<sup>60–62</sup> Since this luminescence is sufficiently intense that it can be directly observed

from Cu-MT in tissue samples,<sup>63</sup> emission spectroscopy provides a powerful technique with which to study the details of Cu(I) binding to metallothionein both *in vitro* and *in vivo*.

Through the extensive series of experiments described above, we have used the luminescence of the copper–thiolate clusters in rabbit liver metallothionein to probe the copper binding site location and metal ion mobility. Our results show an exceptionally strong dependence of the 600-nm emission intensity on the Cu(I):MT molar ratio over the range 1–20. At all temperatures, the emission intensity exhibits a dramatic nonlinear increase in quantum yield as a function of metal added up to 12 Cu(I). Between 12 and 16 Cu(I) the intensity collapses until almost no emission is observed when 20 Cu(I) have been added (Figures 2–4). The emission band center also exhibits a significant red shift between 12 and 16 Cu(I) (Figure 6). The relative emission intensities between the 1st and 12th addition of Cu(I) are highly temperature dependent (Figure 5). At high temperatures (40 °C), almost no increase in intensity is observed in the early stages of the titration (2–7 Cu(I)); whereas, at low temperature (10 °C), the intensity increases with each addition of Cu(I). Long equilibration times at cooler temperatures produce almost the same effect as carrying out the titration at warm temperatures (Figure 10). The effect of warm–cool cycles on the emission intensity is also strongly dependent on the Cu(I):MT molar ratio (Figures 7 and 8). For solutions containing <8 Cu(I), a single warm–cool cycle decreases the emission intensity (Figure 7); whereas for solutions containing between 8 and 12 Cu(I), a single warm–cool cycle increases the emission intensity (Figure 8).

We can interpret the results described above in terms of (i) the initial binding sites of the Cu(I) added to  $\text{Zn}_7\text{-MT}$ , (ii) the mobility of the Cu(I) once bound to the protein and the mobility of the protein backbone itself, (iii) the formation of a specific three-dimensional structure for  $\text{Cu}_{12}\text{-MT}$ , and (iv) the energetically favored state adopted after equilibration. Proteolysis studies of reconstituted Cu(I) metallothioneins have shown that Cu(I) binds preferentially to the  $\beta$  domain.<sup>70,71</sup> Our new emission data now suggest that Cu(I) initially binds across both domains, that is to both  $\alpha$  and  $\beta$ , in a distributed manner at all temperatures. This initial binding is followed by slow redistribution occurring at high temperatures to a domain-specific structure with the Cu(I) binding exclusively in the  $\beta$  domain for  $\text{Cu}_n\text{-MT}$ ,  $n = 1–6$ . Below

(54) Anglin, J. H., Jr.; Batten, W. H.; Raz, A. I.; Sayre, R. M. *Photochem. Photobiol.* 1971, 13, 279–281.

(55) Szymanska, J. A.; Zelazowski, A. J.; Stillman, M. J. *Biochem. Biophys. Res. Commun.* 1983, 115, 167–173.

(56) Stillman, M. J.; Szymanska, J. A. *Biophys. Chem.* 1984, 19, 163–169.

(57) Munger, K.; Lerch, K. *Biochemistry* 1985, 24, 6751–6756.

(58) Munger, K.; Germann, U. A.; Beltramini, M.; Niedermann, D.; Baitella-Eberle, G.; Kagi, J. H. R.; Lerch, K. *J. Biol. Chem.* 1985, 260, 10032–10038.

(59) Mehra, R. K.; Bremmer, I. *Biochem. J.* 1984, 219, 539–546.

(60) Reese, R. N.; Mehra, R. K.; Tarbet, E. B.; Winge, D. R. *J. Biol. Chem.* 1988, 263, 4186–4192.

(61) Byrd, J.; Berger, R. M.; McMillin, D. R.; Wright, C. F.; Hamer, D.; Winge, D. R. *J. Biol. Chem.* 1988, 263, 6688–6694.

(62) Thrower, A. R.; Byrd, J.; Tarbet, E. B.; Mehra, R. K.; Hamer, D. H.; Winge, D. R. *J. Biol. Chem.* 1988, 263, 7037–7042.

(63) Stillman, M. J.; Gasyana, Z.; Zelazowski, A. *J. FEBS Lett.* 1989, 257, 283–286.

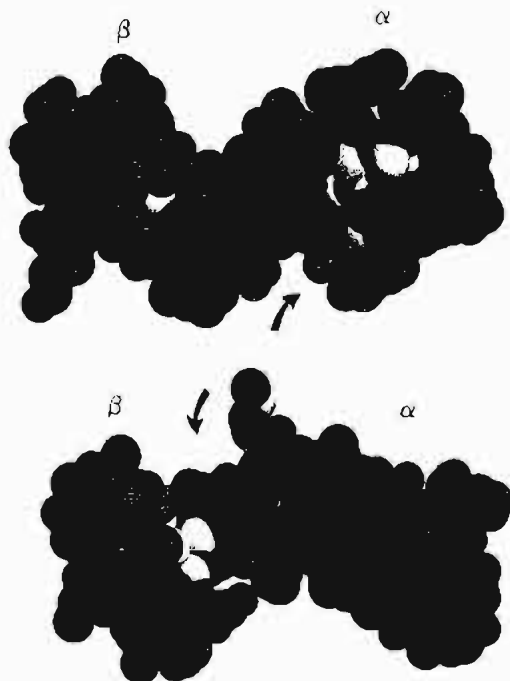


**Figure 11.** Proposed space-filling model of the  $\text{Cu}_{12}$ -MT species produced using the CAChe molecular modeling system based on Allinger's MM2 force field.<sup>64,72</sup> The lightest spheres represent the sulfur contained in the cysteinyl residues. The visibility of these thiolate groups indicates the presence of crevices (shown by the arrows) which provide direct access to the metal-thiolate cores, as described in the text. Full details of the constraints imposed on the modeling and of the computational procedures used can be found in ref 64, as well as the calculated Cu-S bond distances. Using the 3-dimensional structure of  $\text{Cd}_5\text{Zn}_2$ -MT as a guide, metal-free models of the  $\alpha$  and  $\beta$  domains were individually constructed and 6 Cu(I) ions were added to each domain. After energy minimization, the two domains were joined and the entire structure was subjected to further energy minimization. The resulting structure was found to be topologically and sterically possible with each Cu(I) site formulated as a distorted  $[\text{CuS}_3]^{2-}$  trigonal center. Color prints are available from the authors.

we describe how luminescence spectroscopy probes not only the structure of the  $\text{Cu}_{12}$ -MT species but also the occupation of specific sites by Cu(I) and the overall folding of the structure of the molecule.

**Structure of  $\text{Cu}_{12}$ -MT.** The dramatic and highly unusual increase in the quantum yield of emission as 8–12 Cu(I) are added to  $\text{Zn}_7$ -MT suggests the presence of a tight copper-thiolate cluster structure for the  $\text{Cu}_{12}$ -MT species detected by UV-visible absorption and circular dichroism (CD) spectroscopy.<sup>33,64</sup> Our experiments, and those of Winge,<sup>20</sup> in which Chelex-100 resin is used to sequester free metal ions show that no Zn(II) remains in solution after the formation of this species. In Stout's X-ray crystallography studies of  $\text{Cd}_5\text{Zn}_2$ -MT, parts of metal-thiolate clusters are clearly accessible to solvent. In the color plate that displays the space filling models (plate 3.2 in ref 13), both the Zn(II) and Cd(II) metals are visible; therefore, direct localized access to the bound metals by solvent is possible for  $\text{Zn}_7$ -MT and  $\text{Cd}_7$ -MT. However, experimental confirmation of the presence of these crevices in  $\text{Zn}_7$ -MT and  $\text{Cd}_7$ -MT is very difficult. In molecular modeling calculations carried out in this laboratory on the structure of  $\text{Cu}_{12}$ -MT,<sup>64</sup> these same crevices are observed (Figure 11). The size of these crevices must depend on the specific metal-thiolate cluster structure enclosed by the protein. As Cu(I) is added to  $\text{Zn}_7$ -MT, the crevices should open and close as the protein rearranges in order to accommodate the new metal-thiolate structure. The variance in quantum yield as Cu(I) is added indicates a porous binding site and provides the first experimental data that arises as a direct consequence of these

crevices. The presence of crevices which provide direct localized access to the metals by the solvent may be a general feature of the structure of metallothioneins and may explain the facile metal-exchange reactions which have been observed. This is further evidence of the ability of the metallothionein peptide chain to accommodate metals of widely varying sizes while maintaining a similar overall structure as suggested by Messerle et al.<sup>11</sup>

On the basis of these emission results, we propose that  $\text{Cu}_{12}$ -MT has a compact tertiary structure in which the copper-thiolate clusters are protected from general solvent access by the peptide chain. Increases in luminescence intensity due to the protection of the metal center from the solvent environment have been observed in other Cu(I) complexes.<sup>65,66</sup> The stability of the  $\text{Cu}_{12}$ -MT species is shown by the lowering of the electronic ground state energy (indicated by the blue shift in the emission band center at  $\text{Cu}_{12}$ -MT (Figure 6)). The protein backbone prevents larger solvent molecules, such as ethylene glycol, from entering the metal-thiolate clusters which results in an increased emission intensity. Freeze-drying the sample produces a tighter cluster which excludes solvent molecules, greatly enhancing the emission intensity.<sup>67</sup>

The sharp fall in emission intensity with >12 Cu(I) indicates that the cluster structure expands to accommodate the extra metals, dramatically increasing by solvent molecules. We interpret the decrease in emission intensity as being due to the "unwinding" of the binding site until there is 1 Cu(I) bound to each thiolate group in the protein. The increased solvent accessibility to the luminophore is further demonstrated by a change in the lifetime fractional components at this point in the titration ( $\text{Cu(I):MT} > 12$ ).<sup>67</sup> The red shift of the emission band center also indicates that the energy level of the ground state has increased. This may result from a change in the binding geometry of Cu(I) from trigonal to linear or from the ligation of Cu(I) by non-thiolate ligands. Since  $\text{Cu}_{12}$ -MT can be re-formed by adding  $\text{Zn}_7$ -MT to  $\text{Cu}_{20}$ -MT, neither the Cu(I) nor the protein has been oxidized. Oxidation is also ruled out by the fact that the emission spectra of MT species with >12 Cu(I) ions are stable for at least 30 min.<sup>68</sup> Oxidation would result in a rapid decrease in emission signal as the oxidized protein released Cu(I). The emission intensity only decreases when further additions of Cu(I) are made.

**Pathway of Cluster Formation.** What is the pathway of formation of the copper-thiolate clusters in  $\text{Cu}_{12}$ -MT as Cu(I) is added to  $\text{Zn}_7$ -MT? The data in Figure 5 show conclusively that  $\text{Cu}_{12}$ -MT does not form cooperatively. That is, the addition of 1–11 Cu(I) to  $\text{Zn}_7$ -MT does not result in the formation of the stoichiometric amounts of  $\text{Cu}_{12}$ -MT and  $\text{Zn}_7$ -MT. (For example, adding 1 Cu(I) to  $\text{Zn}_7$ -MT does not produce  $1/12$   $\text{Cu}_{12}$ -MT and  $11/12$   $\text{Zn}_7$ -MT.) Similarly, the emission data conclusively show that  $\text{Cu}_6\text{S}_9$  clusters do not form cooperatively. If the binding did occur in a cooperative manner, in each of Figure 5A–C, the normalized emission intensity would be constant since the emission intensity would be directly proportional to the amount of Cu(I) bound. In fact, the emission intensity of  $\text{Zn}_7$ -MT + 12 Cu(I) is much greater than 12 times the intensity of  $\text{Zn}_7$ -MT + 1 Cu(I) (even at 10 °C; Figure 5A) and the emission intensity of  $\text{Zn}_7$ -MT + 6 Cu(I) at 40 °C is much less than 6 times the intensity of  $\text{Zn}_7$ -MT + 1 Cu(I) (Figure 5C).

What structure, then, produces such a low quantum yield for the  $\text{Cu}_6\text{Zn}_4$ -MT species at high temperatures? The data in Figures 5 and 7 show that the emissive properties of  $\text{Cu}_6\text{Zn}_4$ -MT are very temperature dependent. Parallel experiments involving

(64) Presta, A.; Green, A. R.; Zelazowski, A.; Stillman, M. J. Submitted for publication.

(65) Blasse, G.; Breddels, P. A.; McMillin, D. R. *Chem. Phys. Lett.* **1984**, *109*, 24–25.

(66) Dietrich-Buchecker, C. O.; Marnot, P. A.; Sauvage, J.-P.; Kirchoff, J. R.; McMillin, D. R. *J. Chem. Soc., Chem. Commun.* **1983**, 513–515 (Errata: **1984**, 204).

(67) Green, A. R.; Stillman, M. J. Unpublished data.

(68) Green, A. R.; Stillman, M. J. Submitted for publication.

(69) Stillman, M. J.; Zelazowski, A. J. *Biochem. J.* **1989**, *262*, 181–188.

the addition of Cd(II), Ag(I), and Hg(II) to Zn<sub>7</sub>-MT result in the formation of a kinetic product at low temperatures which undergoes irreversible structural changes when heated.<sup>38</sup> We demonstrate here, for the first time, a similar reaction involving Zn<sub>7</sub>-MT and Cu(I). The spectral effects observed in this study clearly arise from the competition between a kinetic and a thermodynamic product.

We explain the dramatic effect of temperature on the relative emission intensities in terms of the rearrangement of the bound metals from a statistical distribution across both domains of MT to a new distribution favoring the  $\beta$  domain. There are many metal binding sites available in metallothionein, and these must be fairly labile if the protein is to be used for metal transport. The temperature dependence of the normalized emission intensities (Figure 5) shows that, at high temperatures, the copper quickly moves to a much less emissive site in the early stages of the titration (2–7 Cu(I)). We will discuss the binding and redistribution of these first seven Cu(I) before going on to describe the changes that arise during the addition of 8–12 Cu(I).

**Binding of 1–7 Cu(I).** As 1–7 Cu(I) are added to Zn<sub>7</sub>-MT at low temperatures (Figures 2 and 5A), the quantum yield per Cu(I) increases reasonably linearly. This is in complete contrast to the trend observed for titrations carried out at 40 °C (Figures 4 and 5C) in which the quantum yield per copper *decreases* as 2–7 Cu(I) are added to Zn<sub>7</sub>-MT. These data, and those summarized in Figure 7, can only be explained if both the  $\alpha$  and  $\beta$  domains fill statistically with Cu(I) over the studied temperature range, followed by a rapid rearrangement of the Cu(I) to the  $\beta$  domain at high temperatures only. CD spectroscopic studies completed in this laboratory on the binding of Cd<sup>2+</sup> to Cu<sub>56</sub>-Zn<sub>24</sub>-MT also support the model that the Cu(I) remains bound in a distributed fashion across both domains at low temperatures as a kinetically controlled product.<sup>64</sup> The detection of the formation of the Cu<sub>6</sub>- $\beta$  domain from the reconstitution of the whole protein with 6 Cu(I) under the relatively harsh conditions of proteolysis<sup>70</sup> indicates that the thermodynamically controlled product of Cu(I) binding to metallothionein involves Cu(I) binding to the  $\beta$  domain.

The differences in the normalized emission intensities for titrations carried out at 10 °C (Figures 2 and 5A) and at 40 °C (Figures 4 and 5C) reflect the rearrangement from the distributed kinetically controlled product to the thermodynamically controlled domain-specific product. The *decrease* in normalized emission intensities at 40 °C (Figure 5C) *must then be caused by Cu(I) binding in the  $\beta$  domain*. At high temperatures, (Zn<sub>4</sub>) <sub>$\alpha$</sub> (Cu<sub>6</sub>) <sub>$\beta$</sub> -MT is formed after equilibration. Subsequent additions of Cu(I) must begin to fill the  $\alpha$  domain, leaving the Cu<sub>6</sub>- $\beta$  domain intact. These additions of Cu(I) cause the emission intensity to rise dramatically under all conditions until 12 Cu(I) have been added. This indicates that, in the whole protein, Cu(I)–thiolate clusters in the  $\alpha$  domain emit more strongly than those in the  $\beta$  domain. The statistical filling at low temperatures results in a linear increase in Cu(I) occupation of both the  $\alpha$  and  $\beta$  domains. Luminescence from the  $\alpha$  domain then dominates the emission spectrum leading to the linear increase in the per copper quantum yield that is observed (Figure 5A). At high temperatures, the increased mobility of the metals (and the protein) causes the less emissive  $\beta$  domain to fill rapidly resulting in almost no increase in emission intensity as 2–7 Cu(I) are added (Figures 4 and 5C).

This increase in Cu(I) mobility as the temperature is raised is probed in the experiments summarized in Figure 7. The data show that the structure of Cu<sub>6</sub>Zn<sub>4</sub>-MT prepared at low temperatures (6 °C) irreversibly changes after being heated to 50 °C. The high-temperature structure dominates once formed.

The changes in emission intensity can be explained as follows. The initial spectrum (a) recorded at 6 °C arises from a statistical distribution of copper in both the  $\alpha$  and  $\beta$  domains. Heating to 50 °C causes Cu(I) to redistribute, filling the  $\beta$  domain which is less emissive (spectrum b). Heating also diminishes the intensity due to the more dominant effects of enhanced solvent deactivation. Although the emission intensity does increase when cooled back to 6 °C (spectrum c) because solvent deactivation is much less efficient (spectrum b to spectrum c), the intensity is significantly lower than the initial spectrum at 6 °C (only 40% of the starting intensity) because the Cu(I) has moved to the  $\beta$  domain (spectrum a to spectrum c). This same pattern is observed up to the addition of 8 Cu(I). To summarize, at low temperatures, the two domains fill equally resulting in a greater Cu(I) occupation of the more emissive  $\alpha$  domain. *The temperature cycle depopulates the  $\alpha$  domain so the final emissive intensity is always lower.*

The experiments shown in Figure 10 emphasize the role of metal mobility in Cu(I) binding to MT. The spectral intensity can be interpreted entirely in terms of the initial and final locations of the Cu(I) (that is, in the  $\beta$  domain, in the  $\alpha$  domain, or in both). The data in the figure show that rearrangement to the domain specific product takes place slowly at 20 °C and rapidly at 40 °C.

This difference in mobility at high and low temperatures can also be used to explain the differences in Zn(II) displacement. Figure 1 shows that Cu(I) displaces Zn(II) almost stoichiometrically at high temperatures between 1 and 5 Cu(I) added (line a), but proportionately more Zn(II) is displaced at low temperatures. Because at high temperatures the Cu(I) rapidly redistributes to fill the  $\beta$  domain, only 3 Zn(II) are displaced by the 6 Cu(I) causing line a to exhibit a stoichiometric slope. When Cu(I) binds in the  $\alpha$  domain, proportionately more Zn(II) will be displaced, as indicated by the low-temperature data in Figure 1. At high temperatures, once 6 Cu(I) have filled the  $\beta$  domain, Cu(I) remains in the  $\alpha$  domain resulting in the sudden drop in Zn(II) concentration from line a to line b.

How general is this result that Cu(I) binds across both domains in Zn<sub>7</sub>-MT before moving to the  $\beta$  domain at high temperatures? The spectroscopic study of Cd(II) binding to Zn-MT also showed this same effect.<sup>38</sup> Later, isolation of  $\alpha$  fragment was shown to be enhanced by the presence of EDTA which was identified as being a carrier for Cd(II) located in protein in which the  $\alpha$  domain was not full.<sup>69</sup> In these two cases, the metal bound to metallothionein is found to be extremely mobile. It seems possible that the exposed edge of the metal binding site provides an unusually open access to the metal–thiolate cluster structure, which in turn allows metal transfer to take place more readily than expected.

**Binding of 8–12 Cu(I).** Figure 5 shows that, at all temperatures, there is a highly unusual increase in the quantum yield of emission as 8–12 Cu(I) are added to Zn<sub>7</sub>-MT: The data can only be explained in terms of the effect of the more emissive  $\alpha$  domain being filled. Figure 8 shows that subjecting cold solutions of Zn<sub>7</sub>-MT containing between 8 and 12 Cu(I) to a single warm-cool cycle produces an unexpected effect. For *all* these solutions, warming reduces the emission intensity (as expected; spectrum b), but recooling (spectrum c) increases the intensity beyond the initial intensity (spectrum a). This can be explained by two factors: (i) the formation at high temperatures of highly emissive species, starting with (Cu<sub>3</sub>Zn<sub>2</sub>) <sub>$\alpha$</sub> (Cu<sub>6</sub>) <sub>$\beta$</sub> -MT and (ii) the mobility of the peptide chain.

The addition of 9 Cu(I) to Zn<sub>7</sub>-MT at high temperatures results in the formation of a highly chiral Cu<sub>9</sub>Zn<sub>2</sub>-MT species (as indicated by the maximization of the Cotton effect at 255 nm in the CD spectrum) which does not form below 24 °C.<sup>64</sup> Since increasing the temperature forces the bound Cu(I) to move to the  $\beta$  domain, this highly optically-active species presumably has the form (Cu<sub>3</sub>Zn<sub>2</sub>) <sub>$\alpha$</sub> (Cu<sub>6</sub>) <sub>$\beta$</sub> -MT. Our data show that the distinct Cu<sub>3</sub>Zn<sub>2</sub> cluster which forms in the  $\alpha$  domain at high temperatures is much more emissive than the structure which results from the

(70) Nielson, K. B.; Winge, D. R. *J. Biol. Chem.* **1984**, *259*, 4941–4946.

(71) Kille, P.; Lees, W. E.; Darke, B. M.; Winge, D. R.; Dameron, C. T.; Stephens, P. E.; Kay, J. *J. Biol. Chem.* **1992**, *267*, 8042–8049.

(72) Allinger, L. N. *J. Am. Chem. Soc.* **1977**, *99*, 8127–8134.

random filling of the  $\alpha$  domain by Cu(I) at low temperatures. The formation of this species also accounts for the hysteresis in Zn(II) loss observed between 8 and 9 Cu(I) added at high temperatures (Figure 1). The formation of  $\text{Cu}_3\text{Zn}_2$  in the  $\alpha$  domain at high temperatures results in pulling the stoichiometric Zn(II) displacement (line **b**) back to the nonstoichiometric fit obtained at cold temperatures.

$^1\text{H}$  NMR spectra<sup>73</sup> indicate an increased influence of the Cu nuclei on the proton nuclei at higher temperatures. This suggests that alterations in the protein backbone occur, possibly extruding solvent molecules from the inner metal-binding cores. We can see evidence of this rearrangement in Figures 8 and 9. Simply adding 12 Cu(I) to  $\text{Zn}_7\text{-MT}$  at low temperatures does not produce the most thermodynamically stable  $\text{Cu}_{12}\text{-MT}$  structure. Although a closed cluster structure is produced giving rise to a large emission intensity (spectrum **a** in Figure 8), the most favorable conformation is not achieved. (It is were, spectrum **a** and spectrum **c** in Figure 8 would have the same intensity since the structure would be exactly the same.) Replacing tetrahedral Zn(II) by trigonal Cu(I) must require major rearrangement of peptide chain which is not possible at 6 °C.<sup>38</sup> Heating the solution to 50 °C causes the emission to decrease (spectrum **b**) as expected due to enhanced solvent deactivation. Warming the solution also causes conformational rearrangement of the protein backbone that tightens the binding site structure such that solvent access is restricted. This results in an enhanced emission intensity when the solution is cooled back to 6 °C (spectrum **c**).

The data in Figure 9 also strongly suggest that the peptide chain plays an important role in the conformation adopted by the metallated protein. In the series of experiments shown in Figure 9A-C,  $\text{Cu}_6\text{Zn}_4\text{-MT}$ ,  $\text{Cu}_9\text{Zn}_2\text{-MT}$ , and  $\text{Cu}_{12}\text{-MT}$  were equilibrated at 50 °C, resulting in domain specific products of  $(\text{Zn}_4)_\alpha$ - $(\text{Cu}_6)_\beta\text{-MT}$ ,  $(\text{Cu}_3\text{Zn}_2)_\alpha(\text{Cu}_6)_\beta\text{-MT}$ , and  $(\text{Cu}_6)_\beta(\text{Cu}_6)_\alpha\text{-MT}$ . With the metals in a "set" location, the emission intensity provides a probe of solvent access to the clustered sites. With no change in conformation of the protein, the intensity should simply rise as the temperature drops due to the reduced solution deactivation. At 6 Cu(I) (Figure 9A), this is almost the case. With 9 and 12 Cu(I), we see a biphasic dependence on temperature (Figures 9B and 9C). Significantly, the effect becomes clearer when the  $\alpha$

domain is completely filled (as shown by the distinct change in the slope at 30 °C in Figure 9C). At this point, the emission from the  $\alpha$  domain is dominating the spectrum. The only interpretation of this effect (at 30 °C) is that solvent access to the  $\alpha$  domain is now blocked. Possible causes for blocking the site are (1) simple conformational rearrangement of the protein backbone that tightens the binding site structure such that solvent access is restricted or (2) protein folding so that the  $\beta$  domain is on top of the crevice in the  $\alpha$  domain resulting in a tighter and less accessible structure. In either case, the peptide chain plays an important role in the structure adopted by metallothionein.

## Conclusions

(1) The emission spectrum of copper metallothionein is a highly sensitive indicator of the location of Cu(I) in the two metal-binding domains of mammalian metallothionein. (2) In the whole protein, Cu(I)-thiolate clusters in the  $\alpha$  domain emit more strongly than those in the  $\beta$  domain allowing the detection of Cu(I) bound in the  $\alpha$  domain by emission spectroscopy. (3) Cu(I) binds to  $\text{Zn}_7\text{-MT}$  in a distributed manner statistically across both domains at all temperatures. (4) At high temperatures the Cu(I) redistributes rapidly to populate the  $\beta$  domain, forming  $\text{Cu}_6(\text{S}_{\text{cys}})_9\text{-}\beta$ , which results in significant reduction in the emission intensity over a period of 5–20 min. (5)  $\text{Cu}_{12}\text{-MT}$  has a tight structure efficiently excluding general solvent access to the two Cu(I)-thiolate clusters. (6) Changes in the emission intensity as a function of temperature suggest that crevices identified from the structure calculated by molecular modeling techniques are present and provide efficient localized access to the metals by the solvent.

**Acknowledgment.** This work was supported financially by Natural Sciences and Engineering Research Council of Canada strategic, operating, and equipment grants (to M.J.S.) and post-graduate scholarships (to A.P. and A.R.G.). We acknowledge the assistance of J. Mack (computer programming) and Dr. A. Zelazowski (preliminary work). We also thank Dr. H. Zinnen and D. Gallagher of CAChe Systems (Tektronix Inc.) for assistance in obtaining the 3-D models of the proposed Cu(I)-thiolate structures of  $\text{Cu}_{12}\text{-MT}$ . M.J.S. is a member of the Center for Chemical Physics and the Photochemistry Unit at UWO. This is publication number 503 of the Photochemistry Unit.

(73) Presta, A.; Stillman, M. J. Unpublished data.